Optical induction scheme for assembling nondiffracting aperiodic Vogel spirals

Falko Diebel, Patrick Rose, Martin Boguslawski, and Cornelia Denz

Citation: Applied Physics Letters **104**, 191101 (2014); doi: 10.1063/1.4875237
View online: http://dx.doi.org/10.1063/1.4875237
View Table of Contents: http://scitation.aip.org/content/aip/journal/apl/104/19?ver=pdfcov
Published by the AIP Publishing

Optical induction scheme for assembling nondiffracting aperiodic Vogel spirals

Falko Diebel,[a] Patrick Rose, Martin Boguslawski, and Cornelia Denz
Institut für Angewandte Physik and Center for Nonlinear Science (CeNoS), Westfälische Wilhelms-Universität Münster, 48149 Münster, Germany

(Received 24 January 2014; accepted 23 February 2014; published online 12 May 2014)

We introduce an experimental approach to realize aperiodic photonic lattices based on multiplexing of nondiffracting Bessel beams. This holographic optical induction scheme takes advantage of the well localized Bessel beam as a basis to assemble two-dimensional photonic lattices. We present the realization of an optically induced two-dimensional golden-angle Vogel spiral lattice, which belongs to the family of deterministic aperiodic structures. With our technique, a very broad class of photonic refractive index landscapes now becomes accessible to optical induction, which could not be realized with established distributed holographic techniques. © *2014 AIP Publishing LLC*. [http://dx.doi.org/10.1063/1.4875237]

The ability to control light propagation by tailoring photonic band gap (PBG) materials has attracted a lot of attention within the last decades, and research activities in this context have led to many groundbreaking developments in different fields of optics.[1] By designing the optical response properties of materials, such as photonic crystals, photonic band gaps arise, which can be regarded as the key requirement for numerous exciting effects and applications, e.g., promising band gap optical waveguides, lasing devices, and gap solitons in photonic lattices.[2–4]

Photonic crystals usually show a high amount of symmetry, and a large spatial refractive index contrast is required to result in a complete photonic band gap. Quasiperiodic photonic lattices with higher rotational symmetries are known to offer more isotropic band diagrams.[5] Moreover, considering deterministic aperiodic structures, which show no rotational nor translation symmetries, the realization of complete PBG materials become more readily achievable.[6] This facilitates the construction of artificial materials which affect and control the propagation properties for a wide range of optical modes.

One particular aperiodic pattern that shows an isotropic PBG is the golden angle spiral.[7] This structure belongs to the wider class of Vogel spirals[8] whose remarkable properties have been studied in many different fields of science. In optics, applications range from enhanced light-matter coupling designs[6] and orbital angular momentum encoding[9] to studies about soliton propagation in the nonlinear regime.[10] But due to the lack of both, translational and rotational symmetries, the fabrication of these structures is very challenging and mostly relies on point-by-point methods in only one plane.

For periodic structures, the optical induction method has proven its powerful ability to create a huge variety of linear and nonlinear photonic lattices.[11,12] By illuminating photosensitive materials with a structured light field, a refractive index modulation can be induced, following the beam's intensity distribution. These photonic lattices represent a highly versatile system to study fundamental linear and nonlinear physics in model experiments, confirmed by many convincingly demonstrated phenomena.[13–16] Over time, the structural complexity of the realized photonic lattices was developed from two-dimensional periodic[12,15] to quasi-periodic three-dimensional.[17] Moreover, the realization of multiperiodic superlattices[18–20] as well as defect lattices[21] further proves the flexibility of the optical induction approach and thus paves the way towards exciting effects in complex photonic lattices. However, all these approaches rely on coherent or incoherent superposition of spatially extended nondiffracting beams with a high amount of regularity,[12,22] which makes it impossible to create two-dimensional aperiodic structures. Consequently, we have to further refine this method to be capable of fabricating a wider class of two-dimensional photonic refractive index landscapes.

In this contribution, we present an experimental scheme to optically induce two-dimensional aperiodic photonic lattices based on multiplexing of well localized nondiffracting Bessel beams.[23] In principle, all two-dimensional structures based on single spots, ranging from small clusters of coupled waveguides to complex aperiodic arrangements thereby become accessible to optical induction. This technique describes a paradigm shift from distributed, parallel methods towards a point-wise induction approach and provides a very powerful platform to study the fundamentals of linear and nonlinear light propagation in aperiodic photonic lattices.

The basic idea behind this approach is to approximate each site of the desired structure with the transverse profile of a zero-order nondiffracting Bessel beam, whose transverse position is given by the addressed two-dimensional structure. Thereby, it is crucial to avoid coherent superposition, which will keep the phase relation between the beams and result in an additional transverse intensity modulation due to interference. Consequently, we illuminate the sample with the individually positioned Bessel beams one after the other in a fast sequence, which is repeated multiple times. We utilize that the buildup of the refractive index modulation is accumulative with time, which is one of the properties of the used photorefractive material. For this method, it is important to

[a]Author to whom correspondence should be addressed. Electronic mail: falko.diebel@uni-muenster.de

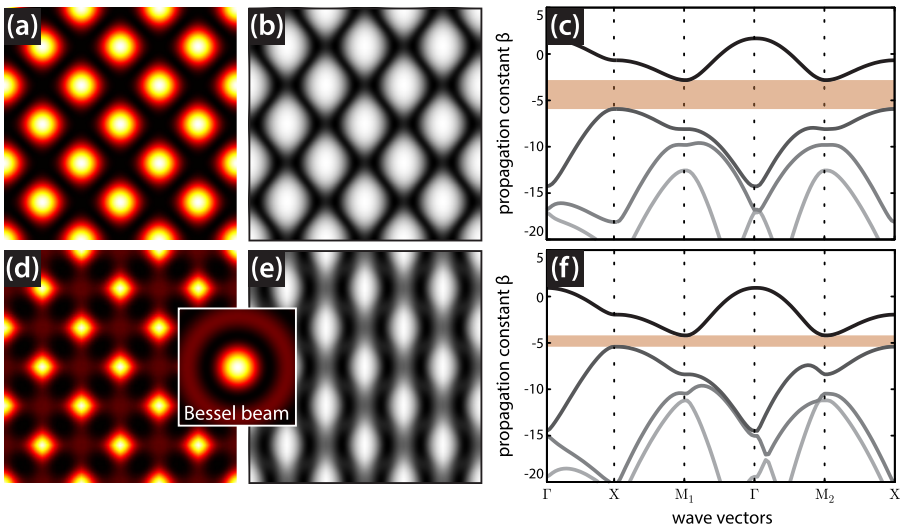

FIG. 1. Comparison between a diamond lattice and its counterpart multiplexed with Bessel beams. (a) Calculated induction beam intensity, (b) resulting anisotropic refractive index modulation, (c) band diagram for the diamond lattice, (d) effective induction beam intensity, (e) calculated index modulation, and (f) band diagram for the case where each lattice site is replaced with the zero-order Bessel beam shown in the inset.

ensure that the illumination time of each Bessel beam is small compared to the typical intensity dependent dielectric relaxation time. For the chosen single beam intensities of approximately 2.2 μW, the relaxation time is in the range of tens of seconds.[18] The presented incremental multiplexing approach is expected to have the same effect on the induced refractive index modulation as a continuous illumination with an effective two-dimensional intensity pattern, which would result from incoherent superposition of all nondiffracting Bessel beams. The simultaneous incoherent superposition of a huge number of beams is also possible in principle, but technically extremely challenging. Therefore, we here rely on incremental multiplexing methods for the optical induction.

To verify that our approach is capable to assemble discrete two-dimensional index structures, we compare a regular diamond lattice with its Bessel beam synthesized counterpart. According to the principle of the proposed induction scheme, each lattice site is replaced by a same-sized (FWHM) zero-order Bessel beam, centered at the corresponding transverse position. In Fig. 1, the induction beam intensities, the calculated index modulations and the band diagram for both cases are shown. Due to the overlapping side lobes of the adjacent Bessel beams, the intensity pattern is slightly reshaped and reduced in contrast. However, this does not remarkably affect the qualitative appearance of the photonic band diagram, as shown in Figs. 1(c) and 1(f). This substantiates the proposed point-wise multiplexing scheme for approximation of many two-dimensional geometries with Bessel beams.

Figure 2 shows a sketch of our setup used to perform the experiments. The beam from a frequency-doubled, continuous-wave Nd:YVO_4 laser emitting at a wavelength of $\lambda = 532\,\text{nm}$ illuminates a high-resolution, programmable phase-only spatial light modulator (SLM). This modulator, in combination with two lenses and a Fourier mask, is used to set up the nondiffracting Bessel beam by addressing a pre-calculated phase pattern onto the SLM. This allows to computer-control every single Bessel beam's position in the transverse plane. Each beam then illuminates a 20 mm long photorefractive $Sr_{0.60}Ba_{0.40}Nb_2O_6$ (SBN:Ce) crystal, which is externally biased with a dc electric field of $E_{\text{ext}} \approx 2000\,\text{V cm}^{-1}$ applied along the optical c-axis. With an imaging lens and a camera mounted on a translation stage, the intensity distribution can be recorded in different transverse planes along the longitudinal axis.

In our scheme, the nondiffracting Bessel beam forms the basic building block for all spatially multiplexed structures. The experimental realization of one single zero-order Bessel beam with a main lobe size of $w \approx 8\,\mu\text{m}$ (FWHM) is shown in Fig. 3. It displays the beam intensity at the front (Fig. 3(a)) and the back face (Fig. 3(b)) of the crystal as well as a scan along the whole crystal length (Fig. 3(d)). In contrast to an equally sized Gaussian beam (Figs. 3(c) and 3(e)), the Bessel beam stays almost unchanged over the whole crystal length of 20 mm and provides a nondiffracting intensity distribution to induce a single two-dimensional waveguide. In the past, the distinguished properties of Bessel beam induced lattices were also employed to demonstrate nonlinear localization and soliton formation.[24,25]

Following the multiplexing idea, the desired structure is induced by illuminating the crystal successively with all Bessel beams, each exposing the crystal for $t = 0.8\,\text{s}$. The whole sequence is repeated 30 times. In the experiment, the corresponding phase-distribution for each Bessel beam at its distinct position is addressed to the SLM, and the respective intensity profile illuminates the photorefractive crystal. In Fig. 4, the basic scheme is exemplarily illustrated for five

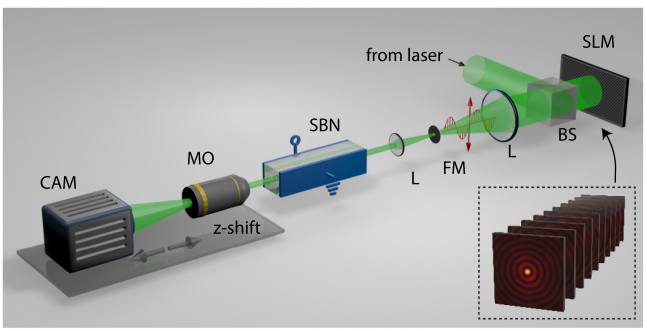

FIG. 2. Experimental setup. BS: beam splitter, FM: Fourier mask, L: lens, MO: microscope objective, SBN: strontium barium niobate crystal, SLM: spatial light modulator. The inset illustrates that different Bessel beams are generated with one SLM.

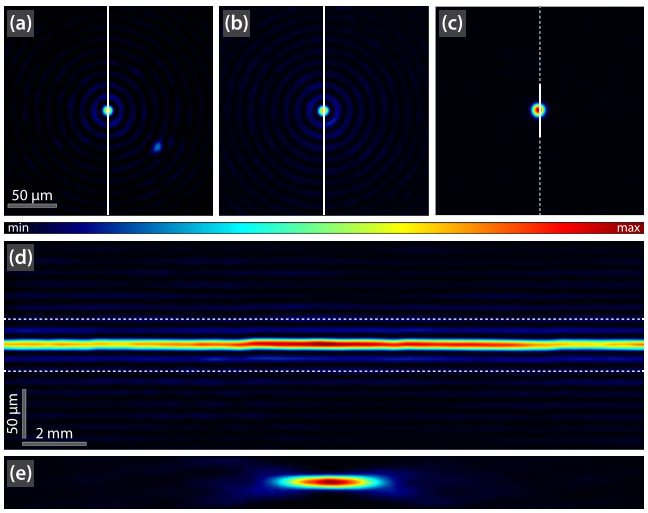

FIG. 3. Nondiffracting Bessel beam. (a) Bessel beam Intensity profile at the front face of the crystal, (b) intensity at the back face, (c) Gaussian beam intensity in the middle of the crystal, (d) nondiffracting intensity of the Bessel beam in longitudinal direction, and (e) diffraction of the same-sized Gaussian beam.

spots forming a two-dimensional cluster of waveguides. The recorded intensity profile for each single Bessel beam is shown in Figs. 4(a)–4(e). Their transverse locations were adjusted to resemble the predetermined structure. The expected effective intensity profile resulting from the multiplexing procedure is shown in Fig. 4(f) as a summation over individually recorded beam intensities.

The multiplexing scheme described in Fig. 4 can readily be scaled up to a considerable number of single waveguides to optically induce even large, complex two-dimensional photonic structures. One comprehensive example of such a structure is given by the Vogel spiral. This spiral belongs to the class of deterministic aperiodic structures and exhibits neither rotational nor translational symmetries. Therefore, it is not easily realizable with known holographic optical induction methods. The construction rule for the Vogel spiral is given by the quantization of the radial and angular variables as $r = r_0\sqrt{n}$ and $\varphi = \alpha n$, with $n = 0 \ldots N$.[6] Here, N is the number of waveguides, r_0 is a scaling factor, and α is an angle which is incommensurable to π. For the

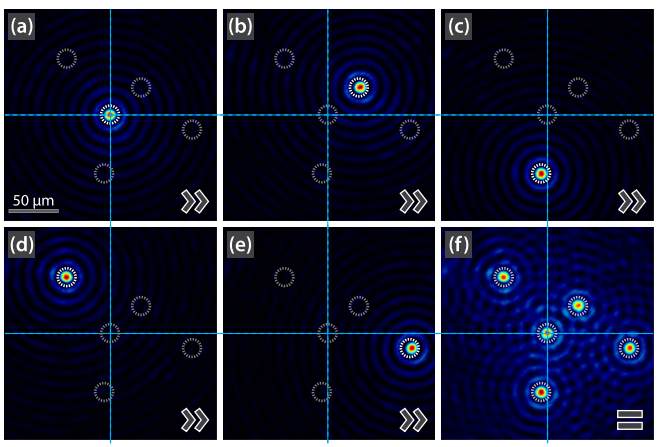

FIG. 4. Scheme of the multiplexing Bessel beam method. (a)–(e) Intensity profiles of the single experimentally realized Bessel beams, and (f) summation over the individually recorded intensities. The circles in the pictures indicate all beam positions.

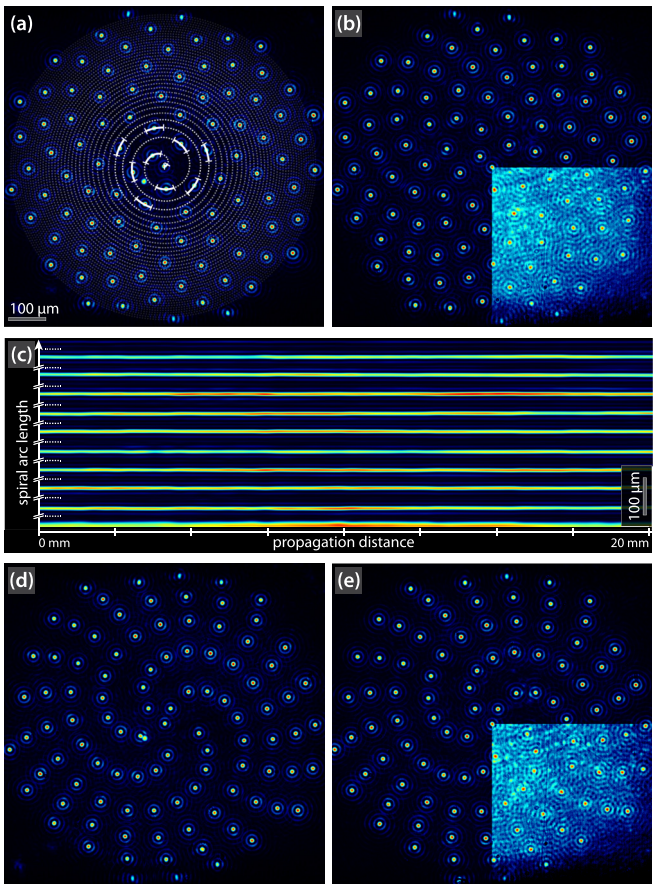

FIG. 5. Two-dimensional Vogel spirals. (a) Digital overlay (with $p = 4$) of the individually recorded Bessel beam intensities forming the golden-angle spiral at the front face of the crystal, (b) corresponding intensity overlay at the back face, (c) unreeled two-dimensional intensity cross-section through the three-dimensional volume along the spiral depicted in (a), (d) intensity overlay for the half-golden-angle spiral at the front face, and (e) at the back face. The insets in (b) and (e) show the digital superposition of the intensities (with $p = 1$).

two cases presented in the following, α is set to be the golden angle and its half, respectively. The golden angle is given by $\Psi = 2\pi/\Phi^2$, where $\Phi = (1 + \sqrt{5})/2$ is the golden ratio, which can also be approximated by Fibonacci numbers f_n as $\Phi = \lim_{n\to\infty} f_n/f_{n-1}$.[6]

In the following, we representatively demonstrate the optical induction of these two types of Vogel spirals with up to $N = 100$ single waveguides. Figure 5 shows the experimental results regarding the realization of the effective induction beam intensity required for the induction of the golden-angle spiral (Figs. 5(a)–5(c)) and the half-golden-angle spiral (Figs. 5(d) and 5(e)). Figures 5(a) and 5(b) show an overlay of the experimentally realized Bessel beam intensities placed at the individual sites of the golden-angle spiral at the front and the back face of the crystal. To highlight the accurate spatial placement of all beams, an overlay (I_{tot}) of all individually recorded intensities (I_n) is shown according to $I_{\text{tot}} = \left(\sum_n I_n^p\right)^{1/p}$, with $p = 4$. The inset in Fig. 5(b) displays the resulting effective intensity profile as a digital summation of all single intensities ($p = 1$).

To verify the nondiffracting nature of this structure in longitudinal direction, the intensity profile along a spiral path in the transverse plane is extracted from the recorded

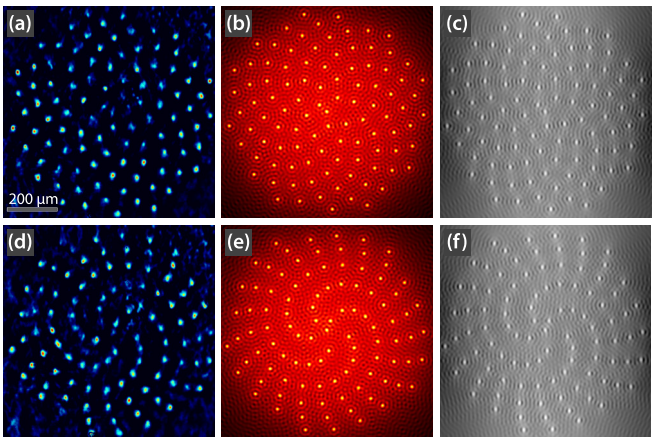

FIG. 6. Optically induced refractive index modulation. (a) and (d) Recorded intensity distribution at the back face of the crystal for a plane wave propagated through the golden-angle and the half-golden-angle spiral, respectively, (b) and (e) corresponding numerically calculated effective intensities, and (c) and (f) calculated refractive index modulations.

three-dimensional intensity volume. This spiral, shown as a path in Fig. 5(a), is given by the construction rule of the Vogel spiral and thus intersects all intensity peaks. For the first 10 Bessel beams along the spiral, the intensity values are unreeled into the two-dimensional map displayed in Fig. 5(c). It clearly verifies that the 8 μm wide beams propagate without spreading or changing their relative distances over a length of 20 mm. This feature is crucial to optically induce effective two-dimensional photonic structures.

Moreover, we demonstrate that the desired aperiodic two-dimensional photonic refractive index structure is actually realized for both cases of Vogel spirals. After inducing the particular structure into the photorefractive SBN crystal, we illuminate the front face with a plane wave and record the intensity pattern at the back face. The imprinted refractive index modulation redistributes the initially homogeneous field intensity to be locally increased at regions of higher refractive index compared to the surrounding. Thus, the recorded intensity map of the guided plane wave at the back face qualitatively resembles the induced refractive index modulation.[26] In Figs. 6(a) and 6(d), the experimentally obtained results are shown for the realized Vogel spirals. They show that in both cases the refractive index modulation accurately follows the effective intensity distribution the crystal is exposed with.

To substantiate our experimental results, we numerically calculated the refractive index modulation induced with these particular intensity distributions in the full anisotropic model.[27] This model well describes the process of optical induction in biased photorefractive crystals such as SBN. Starting with calculating the intensity pattern for the single Bessel beams at the different locations and adding their intensities to the effective intensities shown in Figs. 6(b) and 6(e), we end up with the calculated refractive index modulations for the golden-angle spiral (Fig. 6(c)) and the half-golden-angle spiral (Fig. 6(f)). The simulation of the induced refractive index modulation shows good agreement with the experimentally obtained results, represented by the recorded intensity pattern for the plane wave propagated through the induced photonic structure.

In summary, we have introduced a holographic optical induction scheme for the fabrication of a wide class of two-dimensional photonic lattices, including deterministic aperiodic structures which cannot be fabricated with existing induction techniques. We have demonstrated the capabilities of this multiplexing approach by realizing both, a two-dimensional golden-angle and a half-golden-angle Vogel spiral. Additionally, the precise control over the transverse position as well as the nondiffracting propagation of the well localized zero-order Bessel beams were proven by recording the effective induction beam intensity in different transverse planes along the crystal. Finally, we experimentally showed that the photonic Vogel spiral structure was optically induced, and we compared these results with numerical simulations. This general approach is not limited to the presented structures, and it has the potential to substantially advance future research in modern photonics.

[1]J. D. Joannopoulos, S. G. Johnson, J. N. Winn, and R. D. Meade, *Photonic Crystals: Molding the Flow of Light*, 2nd ed. (Princeton University Press, 2008).
[2]P. Russell, Science **299**, 358 (2003).
[3]H.-G. Park, S.-H. Kim, S.-H. Kwon, Y.-G. Ju, J.-K. Yang, J.-H. Baek, S.-B. Kim, and Y.-H. Lee, Science **305**, 1444 (2004).
[4]P. Rose, T. Richter, B. Terhalle, J. Imbrock, F. Kaiser, and C. Denz, Appl. Phys. B **89**, 521 (2007).
[5]P.-T. Lee, T.-W. Lu, J.-H. Fan, and F.-M. Tsai, Appl. Phys. Lett. **90**, 151125 (2007).
[6]L. Dal Negro and S. Boriskina, Laser Photonics Rev. **6**, 178 (2012).
[7]M. E. Pollard and G. J. Parker, Opt. Lett. **34**, 2805 (2009).
[8]H. Vogel, Math. Biosci. **44**, 179 (1979).
[9]L. Dal Negro, N. Lawrence, and J. Trevino, Opt. Express **20**, 18209 (2012).
[10]Y. V. Kartashov, V. A. Vysloukh, and L. Torner, Opt. Lett. **38**, 190 (2013).
[11]N. K. Efremidis, S. Sears, D. N. Christodoulides, J. W. Fleischer, and M. Segev, Phys. Rev. E **66**, 046602 (2002).
[12]P. Rose, M. Boguslawski, and C. Denz, New J. Phys. **14**, 033018 (2012).
[13]T. Schwartz, G. Bartal, S. Fishman, and M. Segev, Nature **446**, 52 (2007).
[14]H. Trompeter, W. Krolikowski, D. Neshev, A. S. Desyatnikov, A. A. Sukhorukov, Y. S. Kivshar, T. Pertsch, U. Peschel, and F. Lederer, Phys. Rev. Lett. **96**, 053903 (2006).
[15]J. W. Fleischer, M. Segev, N. K. Efremidis, and D. N. Christodoulides, Nature **422**, 147 (2003).
[16]B. Terhalle, T. Richter, K. J. H. Law, D. Göries, P. Rose, T. J. Alexander, P. G. Kevrekidis, A. S. Desyatnikov, W. Krolikowski, F. Kaiser, C. Denz, and Y. S. Kivshar, Phys. Rev. A **79**, 043821 (2009).
[17]J. Xavier, M. Boguslawski, P. Rose, J. Joseph, and C. Denz, Adv. Mater. **22**, 356 (2010).
[18]P. Rose, B. Terhalle, J. Imbrock, and C. Denz, J. Phys. D: Appl. Phys. **41**, 224004 (2008).
[19]M. Boguslawski, A. Kelberer, P. Rose, and C. Denz, Opt. Express **20**, 27331 (2012).
[20]M. Boguslawski, A. Kelberer, P. Rose, and C. Denz, Opt. Lett. **37**, 797 (2012).
[21]A. Kelberer, M. Boguslawski, P. Rose, and C. Denz, Opt. Lett. **37**, 5009 (2012).
[22]Z. Bouchal, Czech. J. Phys. **53**, 537 (2003).
[23]J. Durnin, J. J. Miceli, and J. H. Eberly, Phys. Rev. Lett. **58**, 1499 (1987).
[24]R. Fischer, D. N. Neshev, S. Lopez-Aguayo, A. S. Desyatnikov, A. A. Sukhorukov, W. Krolikowski, and Y. S. Kivshar, Opt. Express **14**, 2825 (2006).
[25]X. Wang, Z. Chen, and P. G. Kevrekidis, Phys. Rev. Lett. **96**, 083904 (2006).
[26]B. Terhalle, D. Träger, L. Tang, J. Imbrock, and C. Denz, Phys. Rev. E **74**, 057601 (2006).
[27]A. A. Zozulya and D. Z. Anderson, Phys. Rev. A **51**, 1520 (1995).